

Correspondence and requests for materials should be addressed to Prof. J. A. J. van Erp, Department of Psychology, University of Amsterdam, PO Box 1570, NL-1007 HH Amsterdam, The Netherlands. E-mail: j.a.j.vanerp@psych.uva.nl.

699

RANKL⁺ data not shown). DcR3-Fc immunoprecipitated shed FasL from FasL-transfected 293 cells (Fig. 2b) and purified soluble FasL (Fig. 2c), as did the Fc-tagged ecto-domain of Fas but not TNFR1. Gel-filtration chromatography showed that DcR3-Fc and soluble FasL formed a stable complex (Fig. 2d). Equilibrium analysis indicated that DcR3-Fc and Fas-Fc bound to soluble FasL with a comparable affinity ($K_d = 0.8 \pm 0.2$ and 1.1 ± 0.1 nM, respectively (Fig. 2e)) and that DcR3-Fc could block nearly all of the binding of soluble FasL to Fas-Fc (Fig. 2e, inset). Thus, DcR3 competes with Fas for binding to FasL.

To determine whether binding of DcR3 inhibits FasL activity, we tested the effect of DcR3-Fc on apoptosis induction by soluble FasL in Jurkat T leukaemia cells, which express Fas (Fig. 3a). DcR3-Fc and Fas-Fc blocked soluble-FasL-induced apoptosis in a similar dose-dependent manner, with half-maximal inhibition at $\sim 0.1 \mu\text{g ml}^{-1}$. Time course analysis showed that the inhibition did not merely delay cell death, but rather persisted for at least 24 hours (Fig. 3b). We also tested the effect of DcR3-Fc on activation-induced cell death (AICD) of mature T lymphocytes, a FasL-dependent process. Consistent with previous results¹, activation of interleukin-2-stimulated CD4-positive T cells with anti-CD3 antibody increased the level of apoptosis twofold, and Fas-Fc blocked this effect substantially (Fig. 3c). DcR3-Fc blocked the

induction of apoptosis to a similar extent. Thus, DcR3 binding blocks apoptosis induction by FasL.

FasL-induced apoptosis is important in elimination of virus-infected cells and cancer cells by natural killer cells and cytotoxic T lymphocytes; an alternative mechanism involves perforin and granzymes [14]. Peripheral blood natural killer cells triggered marked cell death in Jurkat T leukaemia cells (Fig. 3d). DeR3-Ec and Fas-Ec each reduced killing of target cells from ~65% to ~30%, with half-maximal inhibition at ~1 µg ml⁻¹; the residual killing was probably mediated by the perforin-granzyme pathway. Thus, DeR3 binding blocks FasL-dependent natural killer cell activity. Higher DeR3-Ec and Fas-Ec concentrations were required to block natural killer cell activity compared with those required to block soluble FasL activity, which is consistent with the greater potency of membrane-associated FasL compared with soluble FasL [5].

Given the role of immune-cytotoxic cells in elimination of tumour cells and the fact that DcR3 can act as an inhibitor of FasL, we proposed that DcR3 expression might contribute to the ability of some tumours to escape immune-cytotoxic attack. As genomic amplification frequently contributes to tumorigenesis, we investigated whether the DcR3 gene is amplified in cancer. We analysed DcR3 gene copy number by quantitative polymerase chain

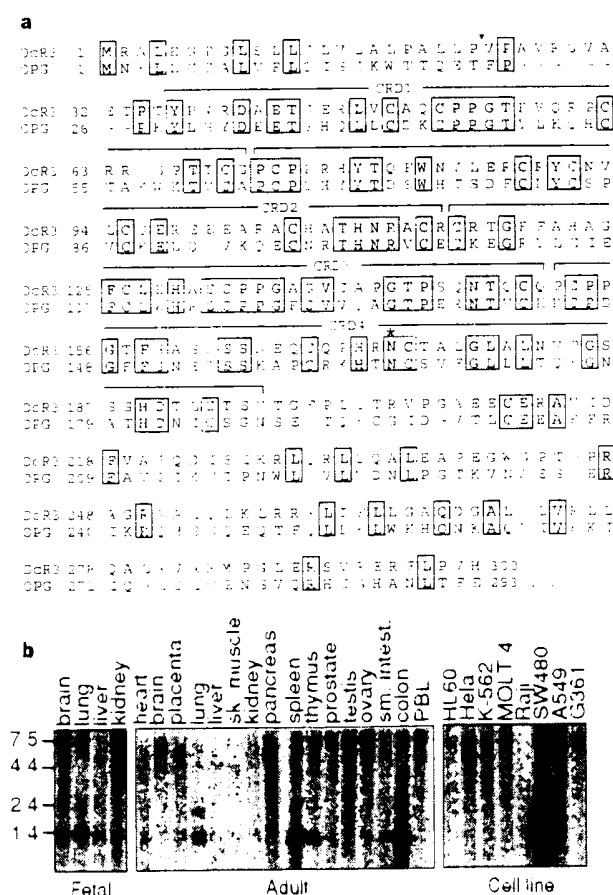


Figure 1 Roman lipoproteins and expression of human DLRP. **a.** Alignment of the amino acid sequences of hDLRP and its sister proteoglycan (DPRG) at the C-terminal 60 residues of DPRG is shown below. The putative signal cleavage site (arrow), the N-glycosylation sequons (N-linked oligosaccharide attachment sites) are indicated. **b.** Expression of hDPRG-mRNA Northern hybridization analysis was done using the DLRP cDNA as a probe and plots of total VAI RNA. Control from normal rats and statin-treated or gender-specific RFLN perlegrin knock-out mice.

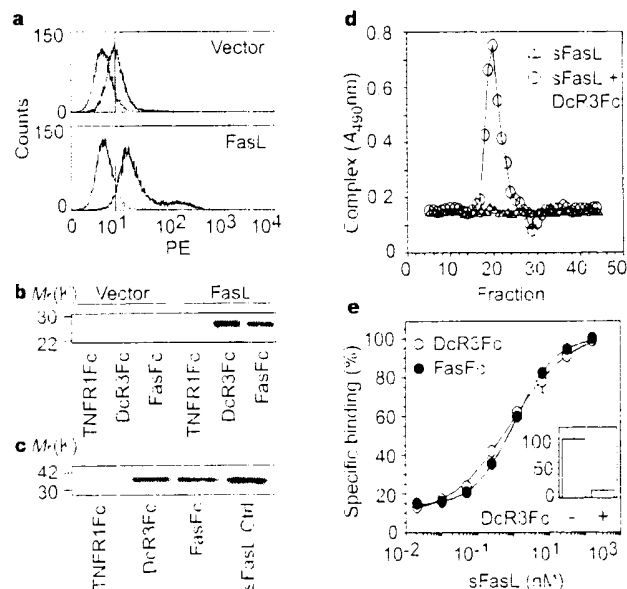


Figure 2 Interaction of DoR3 with FasL. **a**, 293 cells were transfected with pRK5 vector (top) or with pRK5 encoding full-length FasL (bottom), indicated with DoR3-Fc (solid line, shaded area), TNFR1-Fc (dotted line) or buffer control (dashed line). The dashed and dotted lines overlap, and are indicated for binding by FACS. Statistical analysis showed a significant difference ($P < 0.001$) between the binding of DoR3-Fc to cells transfected with FasL or pRK5-RF. In experiments performed in **b**, 293 cells were transfected as in **a** and metabolically labeled, and cell supernatants were immunoprecipitated with Fc-tagged TNFR1, DoR3 or Fas. **c**, Purified soluble FasL (sFasL) was immunoprecipitated with TNFR1-Fc, DoR3-Fc or Fas-Fc, and analyzed with anti-FasL antibody. sFasL was radiolabeled directly for comparison in the rightward lane. **d**, Radiolabeled sFasL was incubated with DoR3-Fc or with buffer and resolved on gel filtration column. Fractions were analyzed in assay that detects complexes containing DoR3-Fc and sFasL-Fc. **e**, Cell surface binding of DoR3-Fc to Fas-Fc or FasL-Fc. FasL-Fc was preincubated with DoR3-Fc with FasL-Fc or sFasL-Fc and radiolabeled sFasL-Fc.

FasL binding; hence, it may represent a third mechanism of extracellular regulation of FasL activity. A decoy receptor that modulates the function of the cytokine interleukin-1 has been described¹. In addition, two decoy receptors that belong to the TNFR family, DcR1 and DcR2, regulate the FasL-related apoptosis-inducing molecule Apo2L^{2,3}. Unlike DcR1 and DcR2, which are membrane associated proteins, DcR3 is directly secreted into the extracellular space. One other secreted TNFR family member is OPG, which shares greater sequence homology with DcR3 (31% than do DcR1 (17%) or DcR2 (19%); OPG functions as a third decoy for Apo2L⁴. Thus, DcR3 and OPG define a new subset of TNFR-family members that function as secreted decoys to modulate ligands that induce apoptosis. Pox viruses produce soluble TNFR homologues that neutralize specific TNF-family ligands, thereby modulating the antiviral immune response⁵. Our results indicate that a similar mechanism, namely, production of a soluble decoy receptor for FasL, may contribute to immune evasion by certain tumours.

Methods

Isolation of DcR3 cDNA. Several overlapping ESTs in GenBank (accession numbers AA025672, AA025673 and W67560) and in LifesecTM (Incyte Pharmaceuticals; accession numbers 1339238, 1533571, 1533650, 1542861, 1749372 and 2207027) showed similarity to members of the TNFR family. We screened human cDNA libraries by PCR with primers based on the region of EST consensus; fetal lung was positive for a product of the expected size. By hybridization to a PCR-generated probe based on the ESTs, one positive clone (DcR30942) was identified. When searching for potential alternatively spliced forms of DcR3 that might encode a transmembrane protein, we isolated 50 more clones; the coding regions of these clones were identical in size to that of the initial clone (data not shown).

Fc-fusion proteins (immunoconjugates). The entire DcR3 sequence, or the ectodomain of Fas or TNFR1, was fused to the hinge and Fc region of human IgG1, expressed in insect SP9 cells or in human 293 cells, and purified as described²².

Fluorescence-activated cell sorting (FACS) analysis. We transfected 293 cells using calcium phosphate or Effectene (Qiagen) with pRK5 vector or pRK5 encoding full length human FasL⁴ (2 µg), together with pRK5 encoding CrmA (2 µg) to prevent cell death. After 16 h, the cells were incubated with biotinylated DcR3-Fc or TNFR1-Fc and then with phycoerythrin-conjugated streptavidin (GibcoBRL), and were assayed by FACS. The data were analysed by Kolmogorov-Smirnov statistical analysis. There was some detectable staining of vector-transfected cells by DcR3-Fc; as these cells express little FasL (data not shown), it is possible that DcR3 recognized some other factor that is expressed constitutively on 293 cells.

Immunoprecipitation. Human 293 cells were transfected as above, and metabolically labelled with [³⁵S]cysteine and [³⁵S]methionine (0.5 mCi; Amersham). After 16 h of culture in the presence of α-VAD-fmk (10 µM), the medium was immunoprecipitated with DcR3-Fc, Fas-Fc or TNFR1-Fc (5 µg), followed by protein A-Sepharose (Repligen). The precipitates were resolved by SDS-PAGE and visualized on a phosphorimager (Fuji BAS2000). Alternatively, purified, Flag tagged soluble FasL (1 µg; Alexis) was incubated with each Fc fusion protein (1 µg), precipitated with protein A-Sepharose, resolved by SDS-PAGE and visualized by immunoblotting with rabbit anti-FasL antibody (OncoGene Research).

Analysis of complex formation. Flag-tagged soluble FasL (25 µg) was incubated with buffer or with DcR3-Fc (40 µg) for 1.5 h at 24 °C. The reaction was loaded onto a Superdex 200 HR 10/30 column (Pharmacia) and developed with PBS; 0.6-ml fractions were collected. The presence of DcR3-Fc-FasL complex in each fraction was analysed by placing 100 µl aliquots into microtitre wells pre-coated with anti human IgG (Boehringer) to capture DcR3-Fc, followed by detection with biotinylated anti-Flag antibody Bio M2 (Kodak) and streptavidin-horse radish peroxidase (Amersham). Calibration of the column indicated an apparent relative molecular mass of the complex of 420 kD (data not shown), which is consistent with a stoichiometry of two DcR3-Fc homodimers to two soluble FasL homotrimers.

Equilibrium binding analysis. Microtitre wells were coated with anti-human

FasL blocked with 2% BSA in PBS. DcR3-Fc or Fas-Fc was added, followed by serially diluted Flag tagged soluble FasL. Bound ligand was detected with anti-Flag antibody as above. In the competition assay, Fas-Fc was immobilized as above, and the wells were blocked with excess IgG1 before addition of Flag tagged soluble FasL plus DcR3-Fc.

T-cell AICD. CD4⁺ lymphocytes were isolated from peripheral blood of individual donors using anti-CD5 magnetic beads (Milenyi Biotech), stimulated with phytohaemagglutinin (PHA; 2 µg ml⁻¹ for 24 h, and cultured in the presence of interleukin-2 (100 U ml⁻¹ for 5 days. The cells were plated in wells coated with anti-CD3 antibody (Pharmingen) and analysed for apoptosis 16 h later by FACS analysis of annexin V binding of CD4⁺ cells²³.

Natural killer cell activity. Natural killer cells were isolated from peripheral blood of individual donors using anti-CD56 magnetic beads (Milenyi Biotech), and incubated for 16 h with ⁵¹Cr loaded Jurkat cells at an effector-to-target ratio of 1:1 in the presence of DcR3-Fc, Fas-Fc or human IgG1. Target-cell death was determined by release of ⁵¹Cr in effector-target co-cultures relative to release of ⁵¹Cr by detergent lysis of equal numbers of Jurkat cells.

Gene-amplification analysis. Surgical specimens were provided by J. Kern (lung tumours) and P. Quirke (colon tumours). Genomic DNA was extracted (Qiagen) and the concentration was determined using Hoechst dye 33258 intercalation fluorimetry. Amplification was determined by quantitative PCR²⁴ using a TaqMan instrument (ABI). The method was validated by comparison of PCR and Southern hybridization data for the Myc and HIF-2 oncogenes (data not shown). Gene-specific primers and fluo-rogenic probes were designed on the basis of the sequence of DcR3 or of nearby regions identified on a BAC carrying the human DcR3 gene (alternatively, primers and probes were based on Stanford Human Genome Center marker AFM218xe7 (T160), which is linked to DcR3 (likelihood score = 5.4). SHGC-36268 (T159), the nearest available marker which maps to ~500 kilobases from T160, and five extra markers that span chromosome 10. The DcR3-specific primer sequences were 5'-CTTCTTCGCGCAGCGTG-3' and 5'-ATGACGCCGGCAGCAG-3' and the fluo-rogenic probe sequence was 5'-FAM-ACACCATGCGTGCTCAAGCAGAApTAMARA, where FAM is 5-fluorescein phosphoramidite. Relative gene copy numbers were derived using the formula 2^{-ΔCT}, where ΔCT is the difference in amplification cycles required to detect DcR3 in peripheral blood lymphocyte RNA compared to test DNA.

Received 14 September; accepted 6 November 1999

1. Nagata, S. Apoptosis by death factor. *Cell* **88**, 3-6 (1997).
2. Smith, C. A., Ferrarini, T. & Goodwin, R. G. The TNF receptor superfamily: cell death and viral proteins: activation, costimulation and death. *Cell* **76**, 459-462 (1994).
3. Simonet, W. S. *et al.* Osteoprotegeron, a novel secreted protein involved in the regulation of bone density. *Cell* **89**, 309-319 (1997).
4. Ueda, T., Taniguchi, T., Golstein, P. & Nagata, S. Molecular cloning and expression of Fas ligand, a novel member of the TNF family. *Cell* **75**, 1119-1128 (1993).
5. Tenebris, D. *et al.* Human tumor necrosis factor precursor structure, expression and homology to lymphotxin. *Nature* **312**, 724-729 (1984).
6. Pitti, E. M. *et al.* Induction of apoptosis by Apo-2 ligand, a new member of the tumor necrosis factor receptor family. *J. Biol. Chem.* **271**, 12657-12660 (1996).
7. Wiley, S. R. *et al.* Identification and characterization of a new member of the TNF family that induces apoptosis. *Immunity* **3**, 673-681 (1995).
8. Marsters, S. A. *et al.* Identification of a ligand for the death-domain-containing receptor Apo-1. *Curr. Biol.* **8**, 523-528 (1998).
9. Chinnipour, Y. *et al.* TWE-2, a new secreted ligand in the TNF family that weakly induces apoptosis. *J. Biol. Chem.* **272**, 32401-32404 (1997).
10. Wong, B. *et al.* TRANCE is a novel ligand of the TNF family that activates c-Jun N-terminal kinase in T cells. *J. Biol. Chem.* **272**, 2590-2594 (1997).
11. Anderson, D. *et al.* A homologue of the TNF receptor and its ligand enhance T-cell growth and dendritic cell function. *Nature* **390**, 171-174 (1997).
12. Lacey, D. *et al.* Osteoprotegerin is a cytokine that regulates osteoclast differentiation and activation. *Cell* **93**, 105-116 (1998).
13. Freeman, J., Winkler, J., Baumes, L., O'Connell, K. M. & Krammer, P. H. Autocrine T-cell suicide mediated by Apo-1/Fas. *Nature* **373**, 445-449 (1995).
14. Anderson, D. *et al.* TRANCE, a novel TNF-related cytokine, is a costimulatory factor for natural killer cells. *J. Exp. Med.* **181**, 1235-1244 (1995).
15. Meinkens, A. *et al.* Regulation of FasL and FasL expression in TCR cells by cytokines and the involvement of FasL in NK cell-mediated cytotoxicity. *Cell* **9**, 394-404 (1997).
16. Chinnipour, Y. *et al.* Mediators of cell-mediated cytotoxicity. *Cell* **90**, 3-14 (1997).
17. Taniguchi, T., Taniguchi, M. & Nagata, S. Identification of Fas ligand as shedding. *Nature Med.* **4**, 136-140 (1998).
18. Chinnipour, Y. *et al.* Quantitative PCR-based homogeneous assay with fluorescent primers to measure c-jun 2' endogenous amplification. *Ann. Chem.* **43**, 752-758 (1997).
19. Freeman, J. *et al.* Osteoprotegerin is a receptor for the osteolytic agent TRANCE. *J. Biol. Chem.* **273**, 4364-4367 (1998).
20. Lacey, D. *et al.* Osteoprotegerin is a receptor for the osteolytic agent TRANCE. *Nature* **388**, 23-27 (1997).
21. Anderson, D. *et al.* Osteoprotegerin is a novel receptor for the osteolytic agent TRANCE. *Nature* **388**, 23-27 (1997).

12. Kishimoto, A. & Nakamura, M. (1998) Signaling and modulation of G-proteins. *Cell* **281**, 13–22.
13. Asteasanz, V. S., Chantrel, M. Immunoadhesins as research tools and therapeutic agents. *Immunol. Rev.* **96**, 47–66 (1997).
14. Martiny-Bar, L. et al. Activation of epidermal growth factor receptor is dependent on its association with Shc. *Cell* **77**, 1181–1192 (1994).

Acknowledgements: We thank Dr. David Moras for his critical comments and suggestions and Dr. Peter Drenth for his kind assistance.

Correspondence and requests for materials should be addressed to A.W. or to the authors. The GenBank accession number for the HisP cDNA sequence is AF044492.

© 1998 Macmillan Publishers Ltd. All rights reserved. 0950-2688/98 \$10.00

Crystal structure of the ATP-binding subunit of an ABC transporter

Li-Wei Hung^{*}, Iris Xiaoyan Wang[†], Kishiko Nikaido[‡],
Pei-Qi Liu[†], Giovanna Ferro-Luzzi Ames[†] & Sung-Hou Kim^{†*}

^{*} E. O. Lawrence Berkeley National Laboratory, [†] Department of Molecular and Cell Biology, and [‡] Department of Chemistry, University of California at Berkeley, Berkeley, California 94720, USA

ABC transporters (also known as traffic ATPases) form a large family of proteins responsible for the translocation of a variety of compounds across membranes of both prokaryotes and eukaryotes¹. The recently completed *Escherichia coli* genome sequence revealed that the largest family of paralogous *E. coli* proteins is composed of ABC transporters². Many eukaryotic proteins of medical significance belong to this family, such as the cystic fibrosis transmembrane conductance regulator (CFTR), the P-glycoprotein (or multidrug-resistance protein) and the heterodimeric transporter associated with antigen processing (Tap1–Tap2). Here we report the crystal structure at 1.5 Å resolution of HisP, the ATP-binding subunit of the histidine permease, which is an ABC transporter from *Salmonella typhimurium*. We correlate the details of this structure with the biochemical, genetic and biophysical properties of the wild-type and several mutant HisP proteins. The structure provides a basis for understanding properties of ABC transporters and of defective CFTR proteins.

ABC transporters contain four structural domains: two nucleotide-binding domains (NBDs), which are highly conserved throughout the family, and two transmembrane domains¹. In prokaryotes these domains are often separate subunits which are assembled into a membrane-bound complex; in eukaryotes the domains are generally fused into a single polypeptide chain. The periplasmic histidine permease of *S. typhimurium* and *E. coli*^{3–5} is a well-characterized ABC transporter that is a good model for this superfamily. It consists of a membrane-bound complex, HisQMP₂, which comprises integral membrane subunits, HisQ and HisM, and two copies of HisP, the ATP-binding subunit. HisP, which has properties intermediate between those of integral and peripheral membrane proteins⁶, is accessible from both sides of the membrane, presumably by its interaction with HisQ and HisM⁷. The two HisP subunits form a dimer, as shown by their cooperativity in ATP hydrolysis⁸, the requirement for both subunits to be present for activity⁹, and the formation of a HisP dimer upon chemical cross-linking. Soluble HisP also forms a dimer¹⁰. HisP has been purified and characterized in an active soluble form¹¹ which can be reconstituted into a fully active membrane-bound complex¹².

The overall shape of the crystal structure of the HisP monomer is that of an 'L' with two thick arms: arm I and arm II; the ATP-binding pocket is near the end of arm I (Fig. 1). A six-stranded β -sheet ($\beta 3$ and $\beta 8$ – $\beta 12$) spans both arms of the L, with a domain of a α -plus β -type structure ($\beta 1$, $\beta 2$, $\beta 4$ – $\beta 7$, $\alpha 1$ and $\alpha 2$ on one side within arm I, and a domain of mostly α -helices ($\alpha 3$ – $\alpha 9$) on the

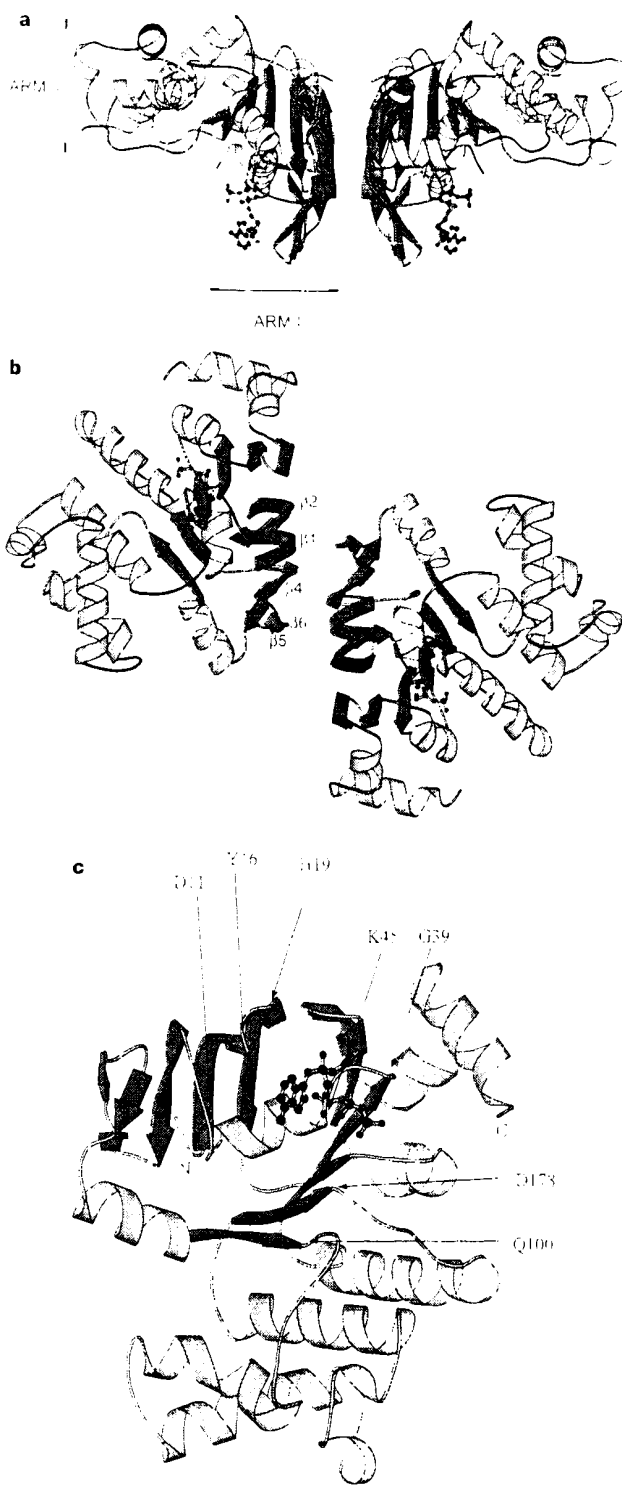


Figure 1 Crystal structure of HisP. **a**, View of the monomer along an axis perpendicular to its two-fold axis. The left and right structures are suggested to face towards the periplasm and cytoplasmic sides, respectively (see text). The thickness of arm I is about 35 Å, comparable to that of membrane α -helices (are shown in orange and β -sheets in green). **b**, View of the two-fold axis of the HisP dimer, showing the relative displacement of the monomers not apparent in **a**. The distance of the inner membrane-embedded view of the monomer from the cytoplasmic side is shown in **a**, towards arm I, showing the ATP-binding pocket. **c**, The ordered and the bound ATP are in orange and green stick representations, respectively. Key residues discussed in the text are indicated in **c**. These figures were prepared with MOLSCRIPT¹³, and rendered using J-3D¹⁴ routines.